OAK RIDGE
NATIONAL LABORATORY
MANAGED BY UT-BATTELLE
FOR THE DEPARTMENT OF ENERGY

ORNL/TM-2000/180/R1

VENUS-2 MOX Core Benchmark: Results of ORNL Calculations Using HELIOS-1.4—Revised Report

R. J. Ellis

Fissile Materials Disposition Program

UT-BATTELLE
ORNL-27 (4-00)

ORNL/TM-2000/180/R1

Computational Physics and Engineering Division

VENUS-2 MOX CORE BENCHMARK: RESULTS OF ORNL CALCULATIONS USING HELIOS-1.4— REVISED REPORT

R. J. Ellis

Date Published: May 2001

Prepared by
OAK RIDGE NATIONAL LABORATORY
Oak Ridge, Tennessee 37831
managed by
UT-BATTELLE, LLC
for the
U.S. DEPARTMENT OF ENERGY
under contract DE-AC05-00OR22725

Page Intentionally Blank

CONTENTS

Page Intentionally Blank

LIST OF FIGURES

Page Intentionally Blank

LIST OF TABLES

VENUS-2 MOX CORE BENCHMARK: RESULTS OF ORNL CALCULATIONS USING HELIOS-1.4—REVISED REPORT

R. J. Ellis

ABSTRACT

The Task Force on Reactor-Based Plutonium Disposition (TFRPD) was formed by the Organization for Economic Cooperation and Development/Nuclear Energy Agency (OECD/NEA) to study reactor physics, fuel performance, and fuel cycle issues related to the disposition of weapons-grade (WG) plutonium as mixed-oxide (MOX) reactor fuel. To advance the goals of the TFRPD, 10 countries and 12 institutions participated in a major TFRPD activity: a blind benchmark study to compare code calculations to experimental data for the VENUS-2 MOX core at SCK-CEN in Mol, Belgium. At Oak Ridge National Laboratory, the HELIOS-1.4 code system was used to perform the comprehensive study of pin-cell and MOX core calculations for the VENUS-2 MOX core benchmark study.

Page Intentionally Blank

1. BACKGROUND

The Task Force on Reactor-Based Plutonium Disposition (TFRPD), now an Expert Group, was formed by the Organization for Economic Cooperation and Development/ Nuclear Energy Agency (OECD/NEA) to provide a forum to address the status and trends of reactor physics, fuel performance, and fuel cycle issues related to the disposition of weapons-grade (WG) plutonium as mixed-oxide (MOX) fuel. The objectives of the TFRPD are to provide current and timely information on core and fuel cycle issues associated with WG plutonium disposition in thermal reactors and fast reactors: core physics and fuel performance and reliability; fuel designs and fuel management techniques for maximizing WG plutonium disposition rates; and the associated fuel handling concerns such as criticality, nuclear and thermal characteristics of spent fuel, and the packaging and transport of fresh and spent fuel. The aim of the Expert Group is to provide the nuclear community with advice on scientific and technical developments necessary to meet the requirements for implementing WG plutonium disposition approaches, especially through the sharing of experimental data and experience.

To fill the TFRPD need for experimental data pertinent for WG MOX validation, data from the MOX core experiment at the VENUS-2 facility in Mol, Belgium, were released by SCK-CEN. The VENUS facility, constructed in the 1960s as a nuclear mockup of a proposed marine reactor, was used in the light-water reactor (LWR) pressure vessel surveillance (PVS) dosimetry improvement program. The VENUS-2 MOX core contained MOX fuel with plutonium isotopics near WG. In a major TFRPD activity, a "blind" benchmark study[1,2] was completed in which more than 10 countries and 12 institutions compared code calculations, including core k_{eff} and extensive pin power distributions, to VENUS-2 MOX core experimental data. The VENUS-2 MOX core benchmark study is also included in the workscope of the OECD/NEA Working Party on the Physics of Plutonium Fuels and Innovative Fuel Cycles (WPPR).

Oak Ridge National Laboratory (ORNL) is involved with the TFRPD activities through the Russian programs of the Fissile Materials Disposition Program (FMDP) under which a major activity is to certify the Russian codes and data for applications involving WG MOX fuel in VVER-1000 reactors. The HELIOS code system has been used widely under this program for verification and validation of Russian methods and data involving both experimental data and calculational exercises. In this role, HELIOS is used as a totally independent calculational system (both in terms of methodology and data) from the Russian methods. This report documents the methods and calculations performed for the ORNL contribution to the OECD/NEA TFRPD VENUS-2 MOX Core Benchmark Study.

Page Intentionally Blank

2. THE VENUS-2 FACILITY

The VENUS critical facility is a "zero power" critical reactor located at SCK-CEN in Mol, Belgium. VENUS is an acronym for "VULCAIN Experimental Nuclear Study;" VULCAIN was the name of a marine reactor concept from the early 1960s.

The central part of the VENUS-2 MOX core consists of UO_2 fuel pins with MOX fuel pins loaded on the periphery of the core (Fig. 1). The VENUS-2 core diagram in Fig. 1 was borrowed from Ref. 1. Figure 2 presents a new diagram of the VENUS-2 core with fuel and poison pin placements more clearly shown. The diagram in Fig. 2 is courtesy of Ref. 2. The VENUS-2 core configuration is called a uranium-plutonium core and is representative of low neutron leakage configurations.

The VENUS-2 core comprises 12 "15 by 15" subassemblies, instead of those of "17 by 17," but the pin-to-pin pitch remains typical of the 17 by 17 subassembly. The central part of the core (four 15 by 15 assemblies) consists of fuel pins 3.3 wt % enriched in ^{235}U. There are 40 Pyrex poison pins in the core. Of the eight assemblies on the periphery of the core, all of which contain fuel pins 4.0 wt % enriched in ^{235}U, eight rows of the most external fuel pins have been replaced by MOX fuel pins (UO_2-PuO_2) enriched 2.0 wt % in ^{235}U and 2.7 wt % in high-grade plutonium with the major plutonium isotopes as shown in Fig. 1. The fuel pin locations can be seen through examination of Fig. 2.

The VENUS-2 experimental results for the core physics study comprise the axial buckling measurement and pin power distribution measurements in 1/8 of the core. Apart from the pin power distribution measurements, reaction rates at several important positions in the reactor were also measured using ^{58}Ni, ^{115}In, ^{103}Rh, ^{64}Zn, ^{237}Np, and ^{27}Al detectors/foils. The VENUS-2 experimental data can be used both for pressure vessel dosimetry studies and core physics analysis, though the latter is the focus of the present reactor physics benchmark calculations and this report.

SCK/CEN-Mol (Belgium)
VENUS-2 LWR-PVS Benchmark Experiment

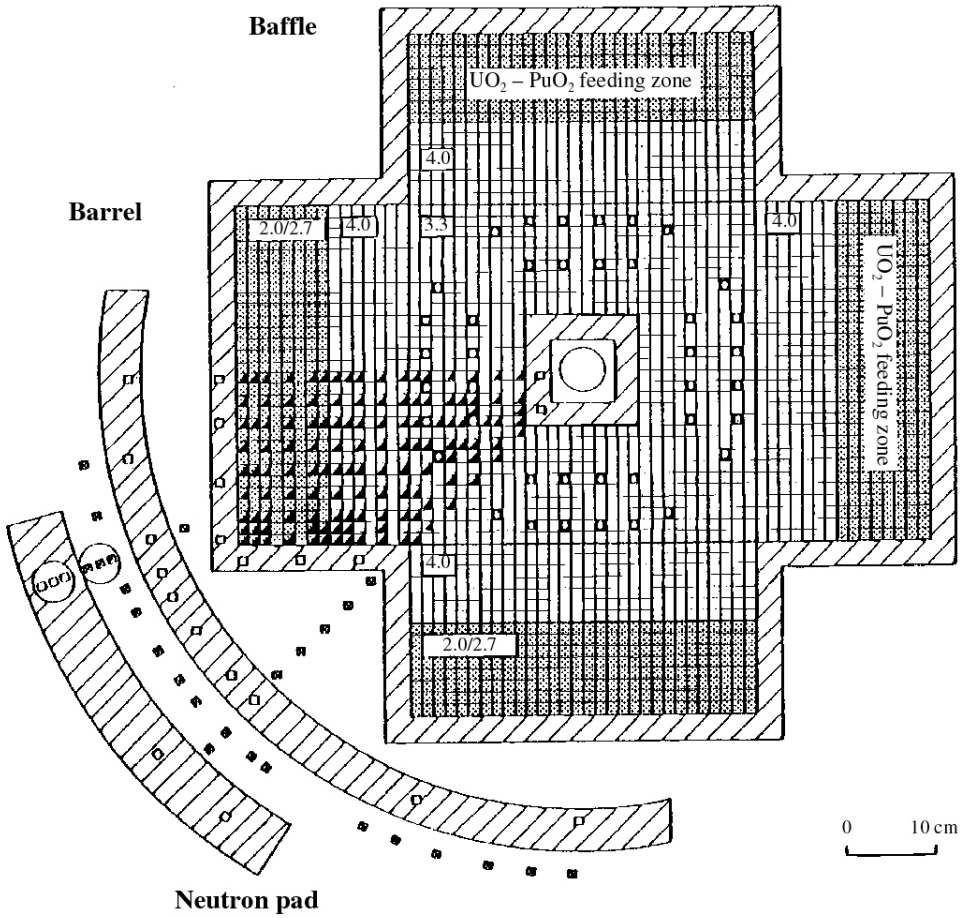

UO_2 – PuO_2 fuel lattice
(Pitch: 1.26 cm)
2.0% uranium enriched
2.7% total plutonium (1)

UO_2 fuel lattice
(Pitch: 1.26 cm)
3.3% and 4.0% uranium enriched

Pyrex rods (2)

Fuel rod measured for determination of power map in the 0-45° sector

Measurement locations in steel structures

Measurement locations in water

Thimble for gamma or neutron spectrometer

(1) Plutonium composition: – 79.37% ^{239}Pu
– 17.14% ^{240}Pu
– 3.05% ^{241}Pu

(2) Amount has been adjusted for criticality

Fig. 1. VENUS-2 facility.

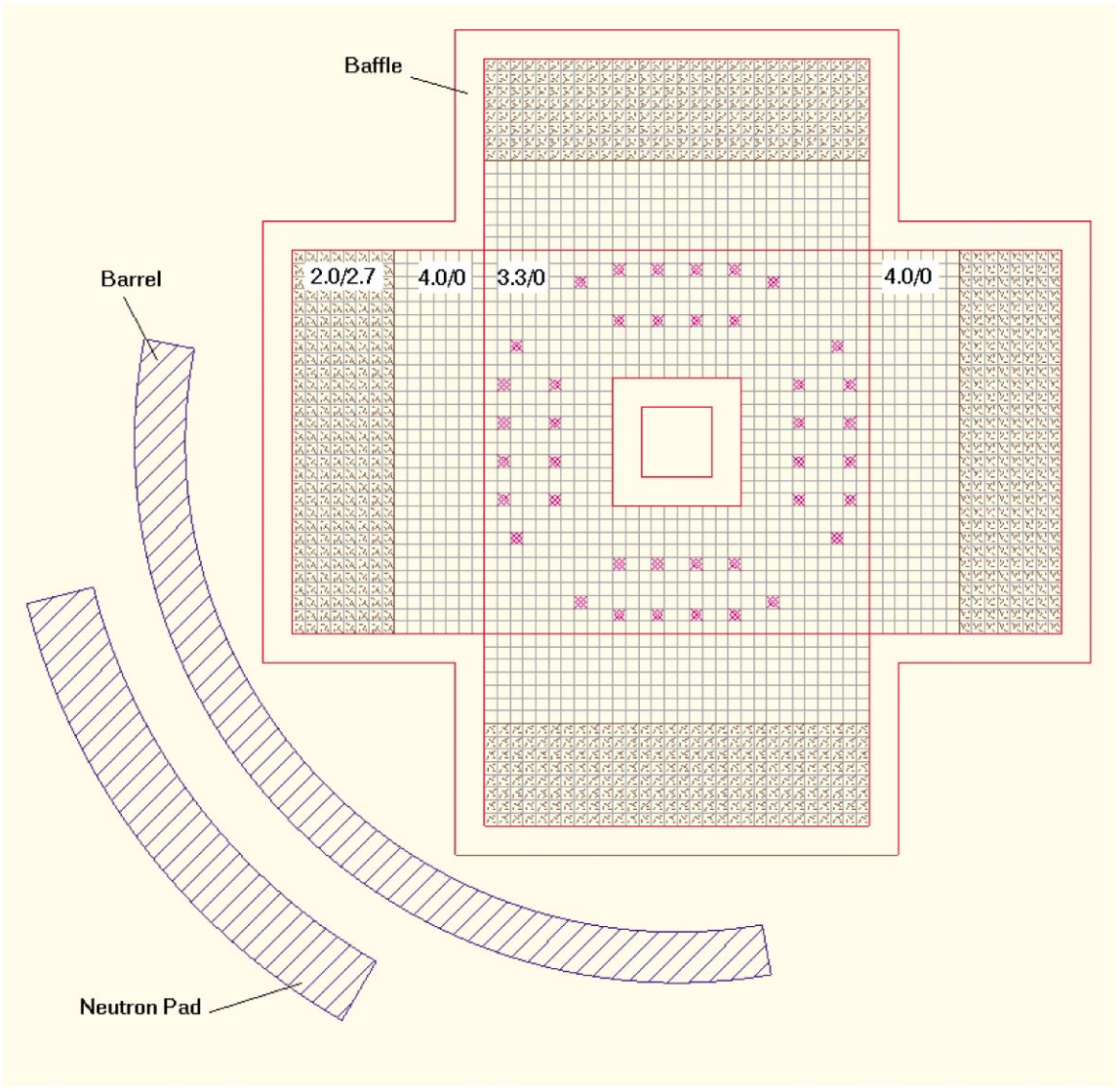

Fig. 2. Details of the VENUS-2 core.

Page Intentionally Blank

3. THE VENUS-2 BENCHMARK STUDY

The objective of the benchmark was to validate and compare the nuclear data sets and production codes used for MOX-fueled system calculations in NEA member countries. The comparison with experimental data would allow identification of discrepancies between calculations and measurements, quantification of the relative merits of the different calculational methods, and possibly identification of the origin of any observed discrepancies.

The VENUS-2 MOX benchmark exercise was a blind test. The measured pin power values at specified VENUS locations were not revealed to the participants. A number of institutions worldwide participated in the benchmark study. The calculated pin power distributions by the diverse computer codes at the different institutions were compared with the experimental results only after all the results were submitted. The computer codes used by the participants included deterministic codes, Monte Carlo codes, and diffusion codes. Various nuclear data sets such as ENDF/B-V, ENDF/B-VI, JEF-1, JEF-2.2, and JENDL-3.2 were also investigated. For power distribution calculations, the deterministic codes included two versions of the collision probability code HELIOS, a collision probability code BOXER, and the two-dimensional (2-D) SN code DORT. The continuous energy Monte Carlo codes were MCNP-4B, MVP, and MCU-B. A diffusion nodal code named GNOMER was also used.

At Oak Ridge National Laboratory (ORNL), the VENUS-2 benchmark calculations were completed using the n,γ-transport lattice physics code HELIOS-1.4. HELIOS[3–5] is a code from Studsvik Scandpower, Inc. The results of the ORNL blind benchmark calculations[6] were delivered to the OECD/NEA before the VENUS-2 experimental data were released to the participants.

The specifications for the VENUS-2 benchmark study and a full description of the core were presented in Ref. 1. The experimental axial buckling measurements were provided for the 2-D calculations. Apart from the geometry and material data, the isotopic concentrations of each medium were also provided to minimize the discrepancies from the atomic density calculations. To obtain vertical bucklings representative of the core, six fuel pins (three at 4.0 wt % and three at 3.3 wt % ^{235}U) were measured axially by gamma-scanning after an irradiation of 8 hours at 90% of the VENUS maximum power. The results requested from the participants hours are summarized as follows:

1. Cell calculations

   For each type of fuel cell (3.3 wt % UO_2, 4.0 wt % UO_2, and 2.0/2.7 wt % MOX), the following are calculated: the k_{inf} values, and the absorption and fission reaction rates per specified isotope (energy integrated and in three groups with 5-keV and 4-eV boundaries). Figure 3 shows the three pin-cell models as prepared for HELIOS for this work.

2. Core calculations

   For the VENUS-2 reactor system, k_{eff} is to be determined. The normalized pin-power distributions (fission rates) are to be determined by pin for 1/8 of the core, including the fuel pins in the diagonal from pin 6 to pin 100 as seen in Fig. 4. Normalization is to be made by OECD/NEA to a core average fission rate = 1 fission/s/fuel pin.

The average fission rate in the core corresponding to the absolute reference irradiation in VENUS-2 is 1.87E+08 fissions/cm/s at the midplane. This average fission rate corresponds to a power level of 595 W. The 128 fuel rods (44 with 3.3 wt % UO_2, 38 with 4.0 wt % UO_2, and 46 with 2.0/2.7 wt % MOX) were assessed after an irradiation of 13.5 hours at 90% of the VENUS maximum power. As mentioned above, the measured pin power values were normalized to a core-averaged fission rate = 1 fission/s/pin (or to a total core fission rate of 2560 fissions/s). The experimental data were taken from the gamma activity of the ^{140}La (fission yields ~6.3% for ^{235}U and ~5.5% for ^{239}Pu, energy ~1.6 MeV, and effective half-life of ~12.8 d).

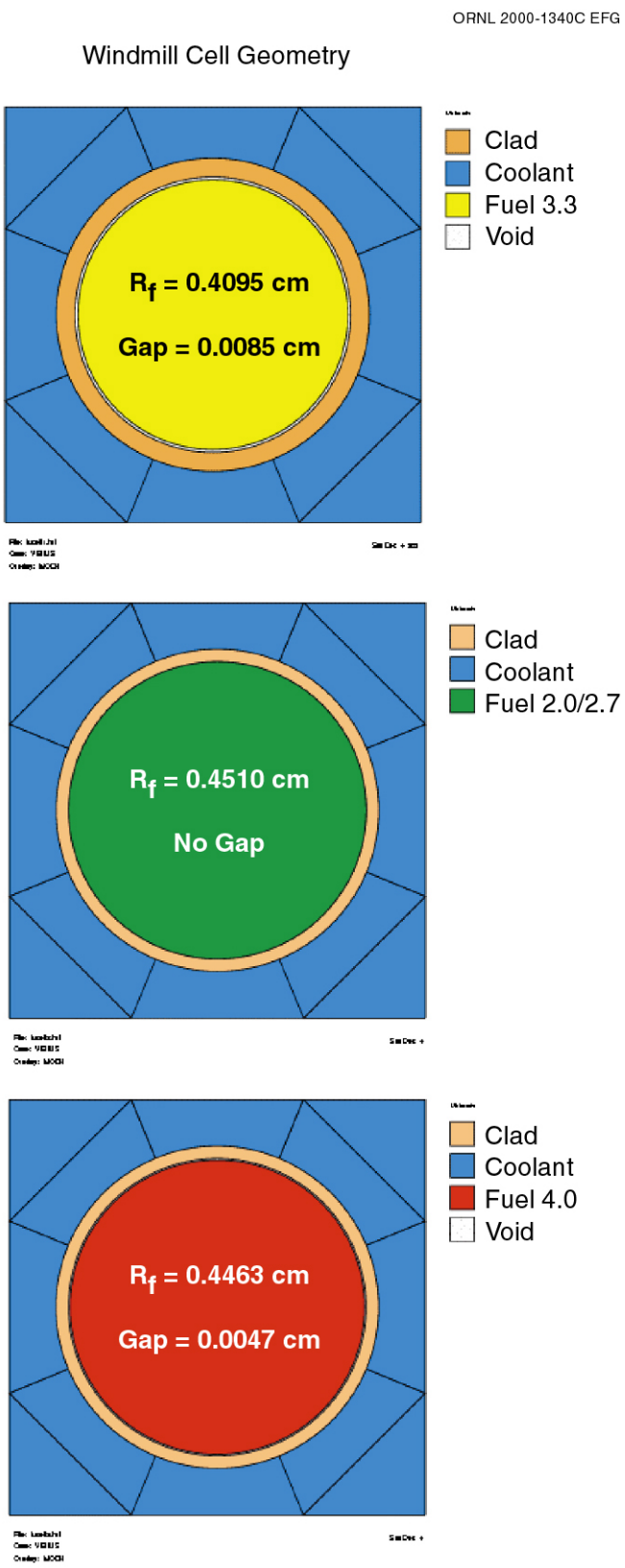

Fig. 3. Pin-cell models.

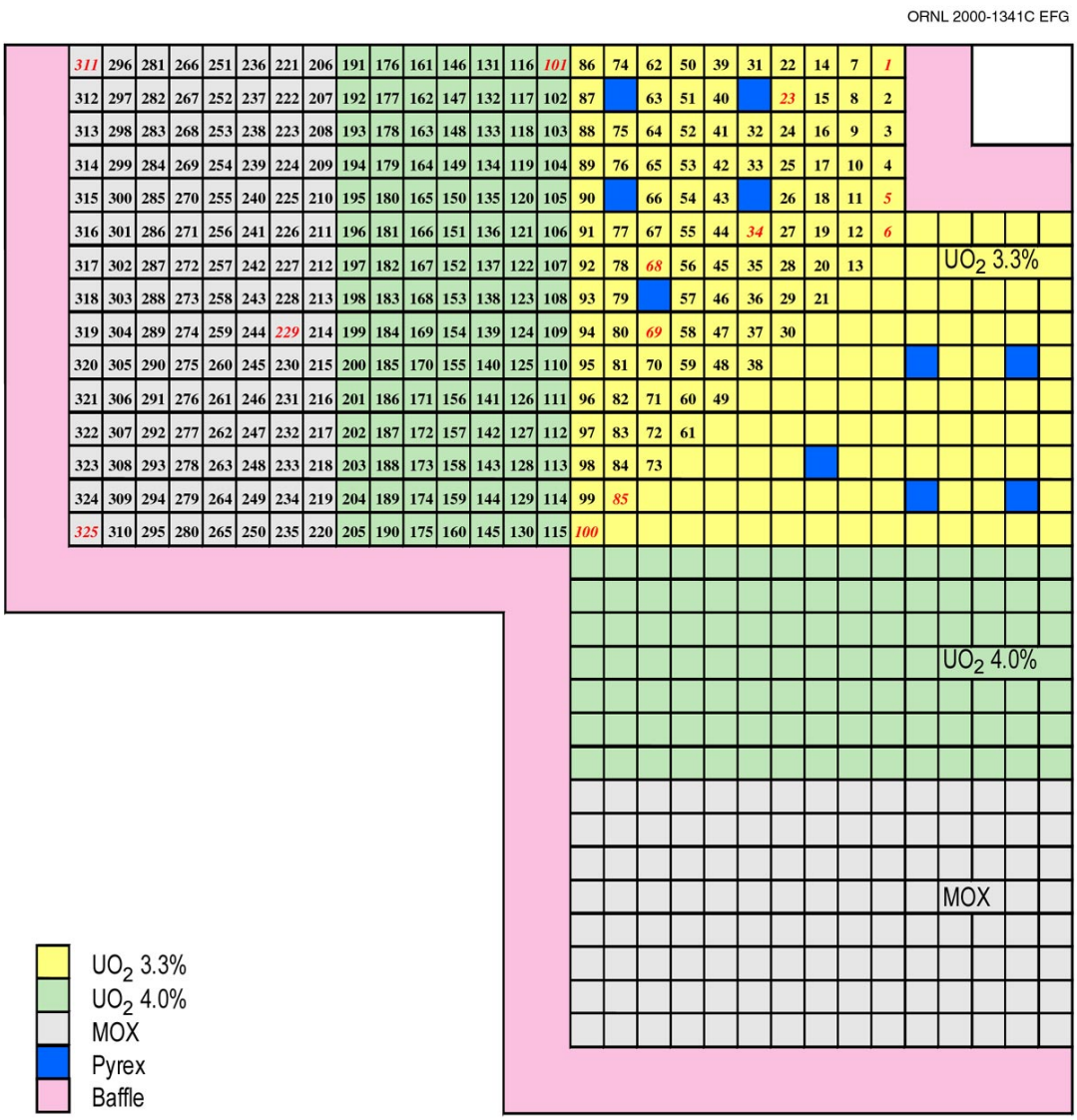

Fig. 4. VENUS pin power locations.

Page Intentionally Blank

4. VENUS-2 HELIOS MODEL DESCRIPTION

For this benchmark study, HELIOS-1.4 was used to model the VENUS-2 reactor system for the core calculations and for the individual fuel pin cells for the cell calculations. For the ORNL results, HELIOS-1.4 was used with nuclear data libraries (based on ENDF/B-VI) in 34-, 89-, and 190-neutron-energy groups. The code uses neutron and γ-transport calculations for lattice physics calculations in a generalized 2-D geometry. Fuel depletion (burnup) can be modeled with HELIOS, but this was not required for the VENUS-2 calculations because of the low power level of the experimental facility. The main calculational method utilized in HELIOS is referred to as CCCP: current coupling between structures and collision probability transport methods within structures.

Table 1 presents the major modeling data for the VENUS-2 reactor system. These data and other information used in the VENUS-2 HELIOS model input are from Ref. 1. The compositions of the materials in the VENUS-2 reactor are presented in Tables 2–4. Table 2 shows the elemental and isotopic (where appropriate) atom densities for the three types of fuel and the Pyrex neutron poison material. Tables 3 and 4 show the elemental compositions of the cladding, water, and reactor structural materials.

The pin cells for the three types of fuel are shown schematically in Fig. 3. In the cell calculations, k_{inf} and the reaction rates requested for three ranges of neutron energies (0–4 eV, 4 eV–5 keV, >5 keV) were calculated for the individual pin-cell models: 3.0 wt % UO_2, 4.0 wt % UO_2, and 2.0/2.7 wt % MOX. The actual energy boundaries used with HELIOS-1.4 were the ones from the nuclear data libraries closest to the specified boundaries. The closest energy boundaries for the HELIOS case were 3.928 eV and 4.881 keV. Small differences can be expected in the reaction rate results from the various codes used in the benchmark study because of small differences in the energy boundaries used.

For the core calculations and the pin power (fission rate) determinations, the 2-D layout of the VENUS-2 system (as shown in Fig. 2) was represented in a HELIOS model as a 1/8-core with specular reflection at the radial boundaries and vacuum boundary conditions at the outer edge. Figure 5 represents the most recent ORNL HELIOS model of VENUS-2. The ORNL VENUS-2 HELIOS model is much more detailed than the resolution in the Fig. 5 diagram permits. For example, the “windmill” cell coolant partition pattern shown in Fig. 3 is used in the modeling for all the fuel pin and Pyrex poison pin sites. Each fuel pin is modeled with four concentric radial zones. The Pyrex poison pins are annular in shape with void in the inner portion. The Pyrex poison region is represented with two annular zones.

Appendix A provides a questionnaire presented to all the benchmark participants. The ORNL (HELIOS) responses are also included. This appendix provides additional information on the modeling methodologies used by ORNL to represent VENUS-2.

Table 1. VENUS-2 modeling details

Variable	Value (in cm unless otherwise indicated)
LEU 3.3 fuel pin	
Fuel radius	0.4095
Inner cladding radius	0.4180
Outer cladding radius	0.4750
LEU 4.0 fuel pin	
Fuel radius	0.4463
Inner cladding radius	0.4510
Outer cladding radius	0.4890
MOX 2.0/2.7 fuel pin	
Fuel radius	0.4510
Inner cladding radius	0.4510
Outer cladding radius	0.4890
Pyrex poison pin	
Inner Pyrex radius	0.3029
Outer Pyrex radius	0.4524
Inner cladding radius	0.4700
Outer cladding radius	0.4890
Pin pitch	1.26
Assembly pitch	23.60
Barrel	
Inner radius	48.283
Outer radius	53.273
Thickness	4.990
Inner and outer baffle wall thickness	2.858
Central square water hole, side	6.884
Axial buckling	2.390E–3 cm^{-2}
Simulated VENUS-2 specific power	9.141E–4 W/gHM

Table 2. Elemental and isotopic concentrations of the VENUS-2 fuel and Pyrex poison materials (atoms/b-cm)

	Fuel 3.3	Fuel 4.0	Fuel 2.0/2.7 (MOX)	Pyrex poison
^{234}U	6.74213E–06	7.17988E–06	3.31550E–06	
^{235}U	7.65322E–04	9.27556E–04	4.13082E–04	
^{236}U	3.68820E–06	5.28177E–06	2.67097E–06	
^{238}U	2.20912E–02	2.18426E–02	1.99605E–02	
^{239}Pu			4.47077E–04	
^{240}Pu			9.61437E–05	
^{241}Pu			1.70372E–05	
^{242}Pu			2.44766E-06	
^{241}Am			4.18948E–07	
O	4.57338E–02	4.55653E–02	4.18853E–02	4.52326E–02
Si				1.74973E–02
^{10}B	3.64042E–09			1.12120E–03
^{11}B	1.46531E–08			4.51296E–03
Al				5.80342E–04
Fe				8.38326E–06
Na				1.48608E–03
K				3.21198E–04

Table 3. Elemental concentrations of the VENUS-2 cladding materials (atoms/b-cm)

	Fuel 3.3 pin cladding	Fuel 4.0 pin cladding	MOX pin cladding	Pyrex pin cladding
C		1.58254E–04	1.58254E–04	1.18827E–04
Mn		1.11582E–03	1.11582E–03	7.53397E–04
P		3.06841E–05	3.06841E–05	4.91240E–04
S		2.22292E–05	2.22292E–05	
Si		2.28418E–04	2.28418E–04	
Cr	7.69688E–05	1.67247E–02	1.67247E–02	1.68355E–02
Ni		8.12063E–03	8.12063E–03	7.70038E–03
Mo		6.53811E–05	6.53811E–05	3.47117E–05
Fe	1.43323E–04	5.95953E–02	5.95953E–02	6.03471E–02
Sn	4.75354E–04			
O	3.00167E–04			
Zr	4.30680E–02			

Table 4. Elemental concentrations of additional VENUS-2 materials (atoms/b-cm)

	Water	Baffle	Barrel
C		2.33752E–04	5.94134E–05
Mn		1.43008E–03	1.12836E–03
P		4.60909E–05	4.30073E–05
S		1.92924E–05	7.41827E-06
Si		4.82892E–04	8.68986E–04
Cr		1.49819E–02	1.68940E–02
Ni		7.06993E–03	8.26696E–03
Mo		2.25187E–04	2.35048E–04
Co		1.11431E–04	7.83050E–05
Fe		6.15902E–02	5.86255E–02
N			2.71726E–04
H	6.68559E–02		
O	3.34279E–02		

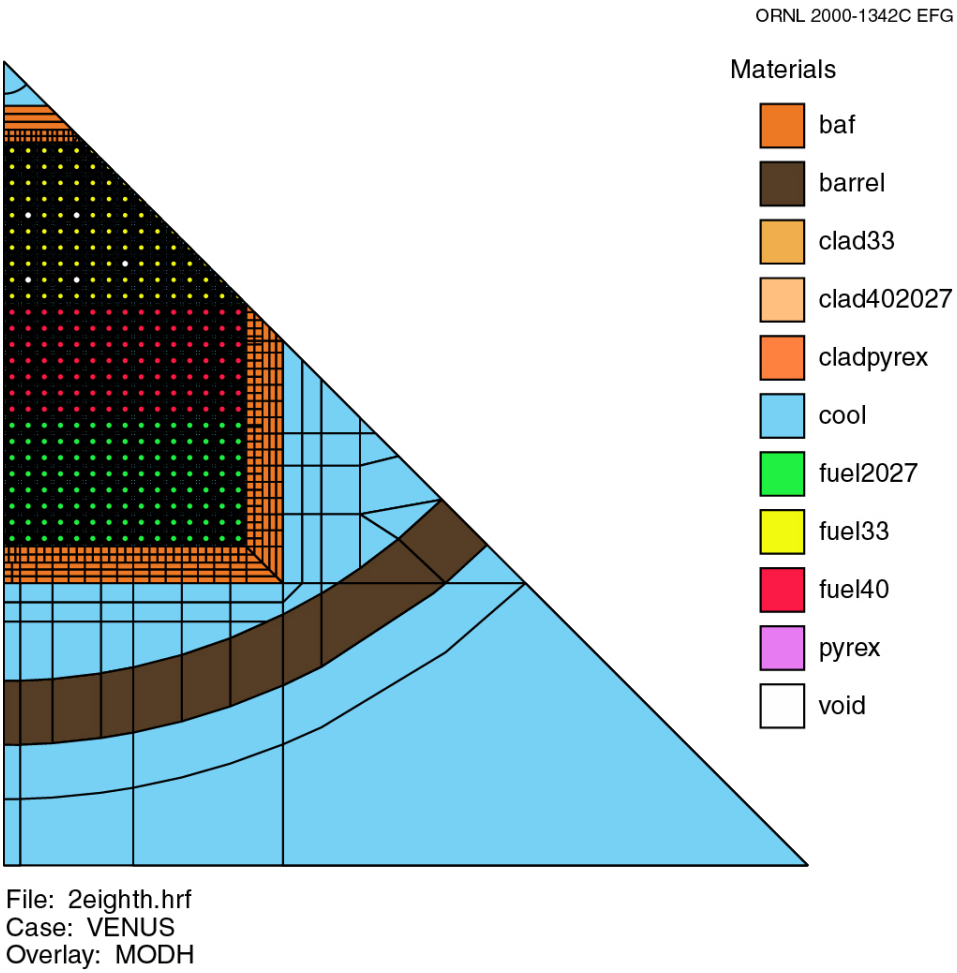

Fig. 5. ORNL HELIOS code model for VENUS-2.

5. RESULTS

5.1 CELL CALCULATIONS

For comparison of the trends related to the number of neutron-energy groups, cell calculations were performed with the 34-, 89-, and 190-neutron-energy group libraries for all three fuel cell types. The complete results are presented in Table 5 for the k_{inf} calculations, as well as for k_{eff} and k_o calculations for a buckling of 2.4×10^{-3} cm^{-2}. The k_{eff} and k_o calculations are shown here for illustrative purposes only because the assumed buckling is not necessarily applicable to infinite arrays of these fuel pin cells. The k_o multiplication factor is the k_{inf} but as calculated in the neutron spectrum corresponding to the input buckling.

Table 5. Cell k determinations as a function of the number of neutron energy groups

Fuel	Number of neutron-energy groups	k_{inf}	k_{eff}	k_o
3.3 wt %	190	1.40847	1.28867	1.40608
	89	1.40677	1.28739	1.40441
	34	1.40698	1.28834	1.40478
4.0 wt %	190	1.34333	1.23504	1.34161
	89	1.34152	1.23366	1.33983
	34	1.34130	1.23391	1.33977
2.0/2.7 wt %	190	1.26254	1.15855	1.26176
	89	1.26279	1.15905	1.26204
	34	1.26496	1.16176	1.26435

In 3.3 and 4.0 wt % fuel, for example, 89- and 34-group results for k_{inf} are similar, and the 190-group result is somewhat higher; for 2.0/2.7 wt % MOX, 190-group and 89-group k_{inf} are similar, and 34G k_{inf} is somewhat higher. Similar trends exist for k_o. Trends in k_{eff} are also different between MOX and LEU pin cells. Overall, the differences in MOX k behavior are probably a result of "plutonium effects" and group-dependent reaction rates.

The 190-group k_{inf} values from ORNL using HELIOS-1.4 were presented to OECD/NEA as the benchmark results. These are isolated in Table 6.

Table 6. The 190-group k_{inf} values

Fuel cell	k_{inf}
3.3 wt % UO_2	1.40847
4.0 wt % UO_2	1.34333
2.0/2.7 wt % MOX	1.26254

Table 7 shows the results for the cell calculations from all of the benchmark participants. These data are from the OECD/NEA final report.[2]

Table 7. The k_{inf} values of cell calculations

Institution	Method	Basic library	UO_2 3.3 wt %	UO_2 4.0 wt %	MOX
NEA	SCALE-4.4 (44g)	ENDF/B-V	1.40385	1.33366	1.25345
KAERI	HELIOS-1.5 (35g)	ENDF/B-VI	1.40904	1.34306	1.26339
ORNL	HELIOS-1.4 (190g)	ENDF/B-VI	1.40847	1.34333	1.26254
PSI	BOXER	JEF-1	1.39636	1.33226	1.26179
SCK-CEN	SCALE-4.4 (238g)	ENDF/B-V	1.39917	1.32829	1.24894
IJS-Trkov	WIMS-D (69g)	JEF-2.2	1.40358	1.33298	1.24858
	WIMS-D (69g)	ENDF/B-VI	1.39840	1.32760	1.24730
NEA+KAERI	MCNP-4B	ENDF/B-VI	1.40479 (±0.00053)	1.33635 (±0.00056)	1.25447 (±0.00061)
JAERI	MVP	JENDL-3.2	1.41115 (±0.00044)	1.34549 (±0.00043)	1.26313 (±0.00051)
Kurchatov Institute	MCU-B	ENDF/B-VI JENDL-3.2 BROND	1.40710	1.33650	1.25490
KFKI	MCNP-4B	ENDF/B-VI	1.40650 (±0.00086)	1.33640 (±0.00088)	1.26310 (±0.001)
GRS	MCNP-4B (square cell)	JEF-2.2	1.41120 (±0.0004)	1.34370 (±0.0004)	1.26140 (±0.0004)
	MCNP-4B (cylindrical cell)	JEF-2.2	1.40950 (±0.0004)	1.34020 (±0.0004)	1.25430 (±0.0004)
IJS-Jeraj	MCNP-4B	ENDF/B-VI	1.40480 (±0.0002)	1.33610 (±0.0002)	1.25470 (±0.0002)

The following Tables 8–31 present fission and absorption rates by specified nuclides for the three fuel pin-cell models for each of the three assigned neutron energy ranges, and the integrated rates over all energies. The OECD/NEA benchmark coordinator will normalize these tabulated rates such that the total fission rate per cell will be 1 fission/s, as presented in Ref. 2.

The first set of tables (Tables 8–19) is for cell calculations with neutron leakage approximated by an axial buckling of 2.4×10^{-3} cm^{-2}. The second set of tables (Tables 20–31) represents the reaction rates for true infinite cell calculations, with no buckling.

Table 8. Energy integrated reaction rates in 2.0/2.7 wt % MOX (reactions/cm^3/s) ($B^2 = 2.4 \times 10^{-3}$ cm^{-2})

	Absorption	Fission
^{234}U	3.6570E+05	1.0154E+04
^{235}U	7.1403E+07	5.6392E+07
^{236}U	1.3013E+05	4.9229E+03
^{238}U	9.5451E+07	1.2245E+07
^{239}Pu	1.7165E+08	1.1283E+08
^{240}Pu	3.4993E+07	3.2684E+05
^{241}Pu	6.9046E+06	5.1946E+06
^{242}Pu	4.5645E+05	6.3531E+03
^{241}Am	1.4801E+05	2.1193E+03

Table 9. Energy integrated reaction rates in 3.3 wt % UO_2 (reactions/cm^3/s) ($B^2 = 2.4 \times 10^{-3}$ cm^{-2})

	Absorption	Fission
^{234}U	6.7993E+05	1.4198E+04
^{235}U	2.1540E+08	1.7821E+08
^{236}U	1.2843E+05	4.5400E+03
^{238}U	8.6857E+07	8.7645E+06

Table 10. Energy integrated reaction rates in 4.0 wt % UO_2 (reactions/cm^3/s) ($B^2 = 2.4 \times 10^{-3}$ cm^{-2})

	Absorption	Fission
^{234}U	7.4626E+05	1.8069E+04
^{235}U	2.1634E+08	1.7646E+08
^{236}U	2.1199E+05	7.7924E+03
^{238}U	9.2756E+07	1.0498E+07

Table 11. Group 1 (E > 5 kV) reaction rates in 2.0/2.7 wt % MOX (reactions/cm^3/s) ($B^2 = 2.4 \times 10^{-3}$ cm^{-2})

	Absorption	Fission
^{234}U	1.3612E+04	9.6131E+03
^{235}U	2.5835E+06	2.1935E+06
^{236}U	5.4583E+03	3.2783E+03
^{238}U	2.3452E+07	1.2245E+07
^{239}Pu	3.1350E+06	2.8058E+06
^{240}Pu	3.9708E+05	3.0783E+05
^{241}Pu	1.3127E+05	1.1925E+05
^{242}Pu	8.2533E+03	6.2709E+03
^{241}Am	2.7516E+03	1.2800E+03

Table 12. Group 1 (E > 5 kV) reaction rates in 3.3 wt % UO_2 (reactions/cm^3/s) ($B^2 = 2.4 \times 10^{-3}$ cm^{-2})

	Absorption	Fission
^{234}U	1.7969E+04	1.2703E+04
^{235}U	3.0985E+06	2.6312E+06
^{236}U	4.8836E+03	2.9350E+03
^{238}U	1.6814E+07	8.7644E+06

Table 13. Group 1 (E > 5 kV) reaction rates in 4.0 wt % UO_2 (reactions/cm^3/s) ($B^2 = 2.4 \times 10^{-3}$ cm^{-2})

	Absorption	Fission
^{234}U	2.3798E+04	1.6665E+04
^{235}U	4.7405E+06	4.0160E+06
^{236}U	8.6837E+03	5.1211E+03
^{238}U	2.0658E+07	1.0498E+07

Table 14. Group 2 (4 eV < E < 5 kV) reaction rates in 2.0/2.7 wt % MOX (reactions/cm^3/s) ($B^2 = 2.4 \times 10^{-3}$ cm^{-2})

	Absorption	Fission
^{234}U	2.8787E+05	2.6684E+02
^{235}U	1.8295E+07	1.1320E+07
^{236}U	1.2134E+05	1.6127E+03
^{238}U	5.9883E+07	0.0000E+01
^{239}Pu	2.1946E+07	1.2758E+07
^{240}Pu	1.8693E+06	1.2437E+04
^{241}Pu	1.5360E+06	1.1653E+06
^{242}Pu	2.0463E+04	8.1635E+01
^{241}Am	1.9874E+04	1.5607E+02

Table 15. Group 2 (4 eV < E < 5 kV) reaction rates in 3.3 wt % UO_2 (reactions/cm^3/s) ($B^2 = 2.4 \times 10^{-3}$ cm^{-2})

	Absorption	Fission
^{234}U	4.0409E+05	3.6413E+02
^{235}U	2.2526E+07	1.3908E+07
^{236}U	1.1552E+05	1.5302E+03
^{238}U	4.5539E+07	0.0000E+01

Table 16. Group 2 (4 eV < E < 5 kV) reaction rates in 4.0 wt % UO_2 (reactions/cm^3/s) ($B^2 = 2.4 \times 10^{-3}$ cm^{-2})

	Absorption	Fission
^{234}U	5.0819E+05	4.7356E+02
^{235}U	3.2688E+07	2.0294E+07
^{236}U	1.9389E+05	2.5827E+03
^{238}U	5.2529E+07	0.0000E+01

Table 17. Group 3 (E < 4 eV) reaction rates in 2.0/2.7 wt % MOX (reactions/cm^3/s) (B^2 = 2.4 × 10^{-3} cm^{-2})

	Absorption	Fission
^{234}U	6.4221E+04	2.7382E+02
^{235}U	5.0525E+07	4.2878E+07
^{236}U	3.3276E+03	3.1874E+01
^{238}U	1.2115E+07	4.7288E+01
^{239}Pu	1.4657E+08	9.7269E+07
^{240}Pu	3.2727E+07	6.5701E+03
^{241}Pu	5.2373E+06	3.9101E+06
^{242}Pu	4.2773E+05	5.3384E-01
^{241}Am	1.2538E+05	6.8328E+02

Table 18. Group 3 (E < 4 eV) reaction rates in 3.3 wt % UO_2 (reactions/cm^3/s) (B^2 = 2.4 × 10^{-3} cm^{-2})

	Absorption	Fission
^{234}U	2.5787E+05	1.1305E+03
^{235}U	1.8978E+08	1.6167E+08
^{236}U	8.0263E+03	7.4869E+01
^{238}U	2.4504E+07	1.0184E+02

Table 19. Group 3 (E < 4 eV) reaction rates in 4.0 wt % UO_2 (reactions/cm^3/s) (B^2 = 2.4 × 10^{-3} cm^{-2})

	Absorption	Fission
^{234}U	2.1427E+05	9.3016E+02
^{235}U	1.7891E+08	1.5215E+08
^{236}U	9.4139E+03	8.8667E+01
^{238}U	1.9569E+07	7.9796E+01

The following tables (Tables 20–31) are for cell calculations with no buckling and represent the infinite pin-cell calculations. Tables 8–19, as discussed previously, present reaction rate results for the cases with nominal bucklings (2.4×10^{-3} cm^{-2}). The results shown in the following infinite cell calculation data are slightly different from those for the corresponding buckled calculations presented previously.

Table 20. Energy integrated reaction rates in 2.0/2.7 wt % MOX (reactions/cm^3/s) (B^2 = 0)

	Absorption	Fission
^{234}U	3.6514E+05	9.8900E+03
^{235}U	7.1473E+07	5.6467E+07
^{236}U	1.2978E+05	4.8305E+03
^{238}U	9.4669E+07	1.1924E+07
^{239}Pu	1.7204E+08	1.1308E+08
^{240}Pu	3.5042E+07	3.1834E+05
^{241}Pu	6.9183E+06	5.2042E+06
^{242}Pu	4.5649E+05	6.1785E+03
^{241}Am	1.4827E+05	2.0857E+03

Table 21. Energy integrated reaction rates in 3.3 wt % UO_2 (reactions/cm^3/s) (B^2 = 0)

	Absorption	Fission
^{234}U	6.7755E+05	1.3808E+04
^{235}U	2.1565E+08	1.7848E+08
^{236}U	1.2754E+05	4.4421E+03
^{238}U	8.6030E+07	8.5145E+06

Table 22. Energy integrated reaction rates in 4.0 wt % UO_2 (reactions/cm^3/s) (B^2 = 0)

	Absorption	Fission
^{234}U	7.4428E+05	1.7585E+04
^{235}U	2.1664E+08	1.7676E+08
^{236}U	2.1095E+05	7.6339E+03
^{238}U	9.1931E+07	1.0206E+07

Table 23. Group 1 (E > 5 kV) reaction rates in 2.0/2.7 wt % MOX (reactions/cm^3/s) (B^2 = 0)

	Absorption	Fission
^{234}U	1.3265E+04	9.3495E+03
^{235}U	2.5268E+06	2.1442E+06
^{236}U	5.3268E+03	3.1895E+03
^{238}U	2.2907E+07	1.1924E+07
^{239}Pu	3.0616E+06	2.7380E+06
^{240}Pu	3.8704E+05	2.9942E+05
^{241}Pu	1.2834E+05	1.1656E+05
^{242}Pu	8.0427E+03	6.0970E+03
^{241}Am	2.6878E+03	1.2447E+03

Table 24. Group 1 (E > 5 kV) reaction rates in 3.3 wt % UO_2 (reactions/cm^3/s) (B^2 = 0)

	Absorption	Fission
^{234}U	1.7445E+04	1.2314E+04
^{235}U	3.0167E+06	2.5607E+06
^{236}U	4.7482E+03	2.8477E+03
^{238}U	1.6360E+07	8.5144E+06

Table 25. Group 1 (E > 5 kV) reaction rates in 4.0 wt % UO_2 (reactions/cm^3/s) (B^2 = 0)

	Absorption	Fission
^{234}U	2.3153E+04	1.6182E+04
^{235}U	4.6277E+06	3.9186E+06
^{236}U	8.4602E+03	4.9745E+03
^{238}U	2.0144E+07	1.0206E+07

Table 26. Group 2 (4 eV < E < 5 kV) reaction rates in 2.0/2.7 wt % MOX (reactions/cm^3/s) (B^2 = 0)

	Absorption	Fission
^{234}U	2.8739E+05	2.6550E+02
^{235}U	1.8214E+07	1.1267E+07
^{236}U	1.2111E+05	1.6090E+03
^{238}U	5.9602E+07	0.0000E+00
^{239}Pu	2.1852E+07	1.2704E+07
^{240}Pu	1.8596E+06	1.2333E+04
^{241}Pu	1.5315E+06	1.1617E+06
^{242}Pu	2.0348E+04	8.1035E+01
^{241}Am	1.9799E+04	1.5555E+02

Table 27. Group 2 (4 eV < E < 5 kV) reaction rates in 3.3 wt % UO_2 (reactions/cm^3/s) (B^2 = 0)

	Absorption	Fission
^{234}U	4.0150E+05	3.6054E+02
^{235}U	2.2316E+07	1.3775E+07
^{236}U	1.1475E+05	1.5194E+03
^{238}U	4.5104E+07	0.0000E+00

Table 28. Group 2 (4 eV < E < 5 kV) reaction rates in 4.0 wt % UO_2 (reactions/cm^3/s) (B^2 = 0)

	Absorption	Fission
^{234}U	5.0609E+05	4.7005E+02
^{235}U	3.2462E+07	2.0149E+07
^{236}U	1.9304E+05	2.5704E+03
^{238}U	5.2156E+07	0.0000E+00

Table 29. Group 3 (E < 4 eV) reaction rates in 2.0/2.7 wt % MOX (reactions/cm^3/s) (B^2 = 0)

	Absorption	Fission
^{234}U	6.4480E+04	2.7496E+02
^{235}U	5.0732E+07	4.3056E+07
^{236}U	3.3393E+03	3.1982E+01
^{238}U	1.2161E+07	4.7480E+01
^{239}Pu	1.4713E+08	9.7641E+07
^{240}Pu	3.2795E+07	6.5840E+03
^{241}Pu	5.2585E+06	3.9259E+06
^{242}Pu	4.2810E+05	5.3591E-01
^{241}Am	1.2578E+05	6.8538E+02

Table 30. Group 3 (E < 4 eV) reaction rates in 3.3 wt % UO_2 (reactions/cm^3/s) (B^2 = 0)

	Absorption	Fission
^{234}U	2.5860E+05	1.1338E+03
^{235}U	1.9032E+08	1.6214E+08
^{236}U	8.0449E+03	7.5034E+01
^{238}U	2.4566E+07	1.0212E+02

Table 31. Group 3 (E < 4 eV) reaction rates in 4.0 wt % UO_2 (reactions/cm^3/s) (B^2 = 0)

	Absorption	Fission
^{234}U	2.1503E+05	9.3358E+02
^{235}U	1.7955E+08	1.5270E+08
^{236}U	9.4420E+03	8.8921E+01
^{238}U	1.9632E+07	8.0074E+01

5.2 CORE CALCULATIONS

The ORNL calculations of k_{eff} are presented for the three libraries (34, 89, and 190 groups) though the definitive value that ORNL reports is the 190-group k_{eff} of 0.99870. Table 32 lists the k_{eff} from all the benchmark participants as presented in the OECD/NEA VENUS-2 report.[2]

Table 32. OECD/NEA VENUS-2 core calculation: ORNL VENUS-2 model for HELIOS

Institution	Code	k_{eff}	Library groups and nuclear data
NEA	DORT	0.99452	44G; ENDF/B-V
KAERI	HELIOS-1.5	0.99817	35G; ENDF/B-VI
SCK-CEN	DORT	0.99233	44G; ENDF/B-V
PSI	BOXER	1.00378	21G; JEF-1, ENDF/B-IV, BROND-2, JENDL-2
IJS-Trkov	GNOMER	0.99450	4G; JEF-2.2
		0.98977	4G; ENDF/B-VI
NEA+KAERI	MCNP4B	1.00213	Continuous energy; ENDF/B-VI
ORNL	HELIOS-1.4	1.00150	34G; ENDF/B-VI
		0.99907	89G; ENDF/B-VI
		0.99870	190G; ENDF/B-VI
KI	MCU-B	0.99650	Continuous energy; ENDF/B-VI, JENDL-3.2, BROND
KFKI	MCNP-4B	1.00050	Continuous energy; ENDF/B-VI, ENDF/B-V
GRS	MCNP-4B	1.00430	Continuous energy; JEF-2.2, ENDF/B-VI, JENDL-3.1, BROND-2.2
IJS-Jeraj	MCNP-4B	0.99570	Continuous energy; ENDF/B-VI, ENDL85, ENDF/B-III

Table 33 presents the ORNL results for the pin fission rates normalized to an average of 1 fission/s/pin. The normalized fission rate values in the table were calculated with HELIOS-1.4 with the 190-group library. The ORNL calculational results were submitted to OECD/NEA as part of the blind benchmark before the experimental VENUS-2 results were released.

In Ref. 2, information was presented to allow the determination of calculated-to-experimental (C/E) pin power ratios. At the TFRPD3 meeting in June 2000, it was revealed that experimental pin power values exist for only some of the pin locations, the other pins had interpolated "experimental" powers assigned to them.

The OECD/NEA final VENUS-2 report will discuss comparisons and trends in the C/E distributions from the results of the various participants. They show good agreement of the ORNL results[2] and in particular, good comparisons to experimental data at the important MOX/LEU and LEU/LEU fuel interfaces.

In Table 34, the ORNL VENUS-2 pin powers are tabulated for a set of representative fuel pins indicated in red lettering in Fig. 4, and the C/E ratios are also shown. Following the delivery of the final ORNL VENUS-2 benchmark results, an improved representation with greater detail was devised for the water between the outer baffle wall and the barrel in the HELIOS VENUS-2 model (as shown in Fig. 5). The calculated pin powers and C/E ratios for the VENUS-2 revised outer model are also presented in Table 34. It is seen that very little changes in most of the pin

Table 33. Calculated pin power (fission rate) distribution

Relative y position (cm)	Relative x position (cm)																						
	–37.17	**–35.91**	**–34.65**	**–33.39**	**–32.13**	**–30.87**	**–29.61**	**–28.35**	**–27.09**	**–25.83**	**–24.57**	**–23.31**	**–22.05**	**–20.79**	**–19.53**	**–18.27**	**–17.01**	**–15.75**	**–14.49**	**–13.23**	**–11.97**	**–10.71**	**–9.45**	**–8.19**	**–6.93**
0.63	0.4257	0.5245	0.6058	0.6821	0.7575	0.8369	0.9350	1.1072	1.0616	1.2006	1.2884	1.3508	1.4020	1.4559	1.5446	1.2461	1.2597	1.3581	1.4005	1.3587	1.2756	1.3218	1.3292	1.2513	1.0423
1.89	0.4227	0.5208	0.6018	0.6779	0.7530	0.8320	0.9299	1.1019	1.0569	1.1959	1.2839	1.3465	1.3980	1.4515	1.5339	1.1940	**Pyrex**	1.3074	1.3887	1.3085	**Pyrex**	1.2749	1.3280	1.2551	1.0445
3.15	0.4187	0.5157	0.5960	0.6715	0.7462	0.8248	0.9223	1.0933	1.0491	1.1877	1.2758	1.3390	1.3914	1.4469	1.5375	1.2416	1.2570	1.3576	1.4026	1.3638	1.2841	1.3346	1.3456	1.2686	1.0524
4.41	0.4123	0.5080	0.5871	0.6617	0.7356	0.8136	0.9103	1.0800	1.0371	1.1751	1.2635	1.3276	1.3814	1.4386	1.5313	1.2385	1.2553	1.3576	1.4051	1.3691	1.2920	1.3480	1.3647	1.2939	1.0779
5.67	0.4038	0.4976	0.5753	0.6486	0.7214	0.7984	0.8941	1.0619	1.0208	1.1579	1.2467	1.3120	1.3677	1.4270	1.5162	1.1857	**Pyrex**	1.3065	1.3959	1.3265	**Pyrex**	1.3178	1.3868	1.3367	1.1528
6.93	0.3931	0.4845	0.5603	0.6321	0.7035	0.7793	0.8736	1.0389	1.0000	1.1359	1.2250	1.2918	1.3501	1.4143	1.5178	1.2380	1.2584	1.3479	1.4083	1.3993	1.3473	1.4059	1.4296	1.3942	1.2980
8.19	0.3803	0.4688	0.5424	0.6122	0.6819	0.7561	0.8487	1.0108	0.9744	1.1087	1.1982	1.2666	1.3280	1.3979	1.5146	1.2624	1.3035	1.2956	1.3903	1.4453	1.4590	1.4715	1.4688	1.4449	
9.45	0.3653	0.4506	0.5215	0.5890	0.6566	0.7288	0.8192	0.9775	0.9440	1.0762	1.1658	1.2359	1.3005	1.3757	1.5008	1.2559	1.2570	**Pyrex**	1.3415	1.4581	1.4923	1.5003	1.4950		
10.71	0.3485	0.4299	0.4977	0.5624	0.6275	0.6974	0.7852	0.9387	0.9084	1.0380	1.1274	1.1990	1.2666	1.3467	1.4802	1.2554	1.3153	1.3082	1.4058	1.4741	1.5023	1.5113			
11.97	0.3300	0.4066	0.4709	0.5325	0.5947	0.6619	0.7464	0.8943	0.8673	0.9935	1.0823	1.1552	1.2256	1.3103	1.4516	1.2473	1.3457	1.3953	1.4435	1.4795	1.5010				
13.23	0.3095	0.3810	0.4413	0.4993	0.5583	0.6222	0.7029	0.8442	0.8204	0.9422	1.0298	1.1034	1.1762	1.2648	1.4118	1.2245	1.3364	1.3993	1.4412	1.4706					
14.49	0.2874	0.3532	0.4090	0.4630	0.5183	0.5785	0.6547	0.7878	0.7669	0.8830	0.9681	1.0417	1.1160	1.2076	1.3577	1.1861	1.3036	1.3720	1.4178						
15.75	0.2642	0.3233	0.3740	0.4237	0.4748	0.5307	0.6014	0.7242	0.7050	0.8128	0.8935	0.9650	1.0394	1.1324	1.2840	1.1304	1.2507	1.3259							
17.01	0.2405	0.2913	0.3362	0.3811	0.4278	0.4787	0.5423	0.6508	0.6300	0.7245	0.7961	0.8614	0.9316	1.0228	1.1746	1.0477	1.1737								
18.27	0.2171	0.2556	0.2935	0.3331	0.3749	0.4202	0.4741	0.5593	0.5251	0.5946	0.6478	0.6962	0.7495	0.8265	0.9749	0.9135									

Table 34. ORNL VENUS-2 pin power calculations with HELIOS-1.4 in 190-group: the effect of an improved outer model

Pin number (see red-labeled pins in Fig. 4)	Reported as part of the benchmark study		Revised outer model	
	Calculated	C/E	Calculated	C/E
1	1.0423	0.965	1.0407	0.964
5	1.1528	1.019	1.1511	1.018
6	1.2980	0.996	1.2960	0.995
23	1.2749	0.994	1.2730	0.993
34	1.3473	0.980	1.3454	0.980
68	1.2956	1.007	1.2939	1.006
69	1.3082	0.977	1.3065	0.976
85	1.1737	0.947	1.1724	0.946
100	0.9135	0.986	0.9126	0.985
101	1.5446	0.989	1.5429	0.988
229	0.7852	0.994	0.7856	0.995
311	0.4257	0.983	0.4356	1.006
325	0.2171	0.969	0.2218	0.990

powers, except at the periphery by the other baffle wall. The C/E ratios for these pins improve considerably.

Table 35 presents the k_{eff} values for 190G, 89G, and 34G HELIOS-1.4 VENUS-2 core calculations for this revised ORNL model compared to the previous official model results as presented in Table 32. The results do not change much (~0.03% reactivity), and the trend to slightly higher k_{eff} with fewer groups is the same as earlier noted.

Table 35. ORNL VENUS-2 core k_{eff} calculations with HELIOS-1.4: effect of improved outer water model

	Reported results	Using revised outer model
190G	0.99870	0.99908
89G	0.99907	0.99942
34G	1.00150	1.00181

Page Intentionally Blank

6. SUMMARY AND CONCLUSIONS

This report documents and presents the ORNL results for the OECD/NEA VENUS-2 MOX core blind benchmark study using HELIOS-1.4. The ORNL results are presented for three pin-cell calculations, and for the VENUS-2 core calculation.

In addition to the official ORNL benchmark results as delivered to OECD/NEA, this report presents some illustrative comparisons with experimental data for VENUS-2 pin powers. Also, the effects of improved modeling of the water region between the baffle wall and the barrel are presented and discussed.

The ORNL pin-cell k_{inf} calculations compare favorably to the results of the other institutions. The ORNL k_{eff} calculation for the VENUS-2 core compares well to the critical experiment. The HELIOS-1.4 k_{eff} determination with the 190-neutron-energy-group library is within 0.1% of critical. There is a small trend observed toward slightly higher values of k_{eff} as the number of groups is reduced to 89 and 34.

Page Intentionally Blank

REFERENCES

1. B. C. Na and E. Sartori, *Blind Benchmark on the VENUS-2 MOX Core Measurements,* NEA/SEN/NSC/WPPR(99)2, OECD/Nuclear Energy Agency, Paris, May 1999.

2. B. C. Na, "Benchmark on the VENUS-2 MOX Core Measurements," NEA/NSC/DOC(2000)7, ISBN 92-64-18276-4, December 2000.

3. R. J. J. Stamm'ler and M. J. Abbate, *Methods of Steady-State Reactor Physics in Nuclear Design,* Academic Press, London, 1983.

4. J. J. Casal, R. J. J. Stamm'ler, E. A. Villarino, and A. A. Ferri, "HELIOS: Geometric Capabilities of a New Fuel-Assembly Program," *Proceedings of the International Topical Meeting on Advances in Mathematics, Computations, and Reactor Physics, Pittsburgh, Pennsylvania, April 28–May 2, 1991,* Vol. 2, p. 10.2.1 1–13.

5. E. A. Villarino, R. J. J. Stamm'ler, and A. A. Ferri, "HELIOS: Angular Dependent Collision Probabilities," *Nuclear Science and Engineering,* **112**(16) (1992).

6. R. J. Ellis, "VENUS-2 Benchmark Calculations: ORNL Results with HELIOS-1.4," Presentations of preliminary and final ORNL results, Task Force On Reactor-Based Plutonium Disposition Meetings: TFRPD2 (November 1999) and TFRPD3 (June 2000), OECD/NEA Data Bank, Paris, France. (The final ORNL results were delivered electronically to the OECD/NEA Data Bank on February 1, 2000.)

Page Intentionally Blank

Appendix A

OECD/NEA SPECIFICATIONS

Page Intentionally Blank

Appendix A. OECD/NEA SPECIFICATIONS

A.1 Appendix 2 from the OECD/NEA Specifications Document

Details to be provided about the Calculational Scheme Used
(preferred format is WORD)

1. Name of participant

2. Establishment

3. Name of Code System(s) Used

4. Bibliographic References for the Codes Used

5. Origin of Cross Section Data (e.g. ENDF/B-VI, JEF-2.2, JENDL-3.2, etc.)
   (describe deviations of standard libraries, e.g. mix from different libraries, details)

6. Spectral Calculations and Data Reduction Methods Used
   (please describe your scheme, through a graph and explanatory words provide details about assumptions made)

   a. resonance shielding: specify method(s) and specify energy range, and the nuclides (actinides, clad, fission products, oxygen, unresolved resonance treatment),

   b. mutual shielding (overlapping of resonances),

   c. fission spectra: specify whether only a single spectrum was used or a weighted mix from all fissile nuclides, explain procedure,

   d. how was the (n,2n) reaction treated?

   e. weighting spectrum for scattering matrices, e.g. correction of the out-scatter and self-scatter terms considering the differences between the original weighting spectrum and realistic cell spectrum.

7. Number of Energy Groups Used in the different phases

8. Cell Calculation

   a. type of calculation: (i.e. heterogeneous, homogeneous),

   b. theory used: (diffusion, transport),

   c. method used; (finite difference, finite elements, nodal, Sn(order), collision probability, Monte Carlo, J+/-, etc.),

   d. calculation characteristics: (meshes, elements/assembly, meshes/pin, number of histories, multi-group, continuous energy, etc.).

9. Other Assumptions and Characteristics

10. Comments Useful for Interpreting correctly the Results

A.2 Response

1. Name of Participant:

Ronald James ELLIS
(ellisrj@ornl.gov)

2. Establishment:

Oak Ridge National Laboratory (ORNL),
Reactor Physics Group,
Nuclear Analysis and Shielding Section,
Computational Physics and Engineering Division,
P.O. Box 2008, Oak Ridge, Tennessee, USA 37831

3. Name of Code System Used:

HELIOS-1.4

4. Bibliographic Reference for the Codes Used:

The following are open-literature references for HELIOS:

—R. J. J. Stamm'ler and M. J. Abbate, *Methods of Steady-State Reactor Physics in Nuclear Design*, Academic Press, London (1983).

—J. J. Casal, R. J. J. Stamm'ler, E. A. Villarino, and A. A. Ferri, "HELIOS: Geometric Capabilities of a New Fuel-Assembly Program," *Proceedings of International Topical Meeting on Advances in Mathematics, Computations, and Reactor Physics, Pittsburgh, Pennsylvania, April 28–May 2, 1991*, Vol. 2, p. 10.2.1 1-13.

—E. A. Villarino, R. J. J. Stamm'ler, and A. A. Ferri, "HELIOS: Angular Dependent Collision Probabilities," *Nuclear Science and Engineering*, Vol. 112, 16 (1992).

5. Origin of the Cross-Section Data:

The nuclear data libraries used were prepared by Studsvik Scandpower Inc. for 34 groups, 89 groups, and 190 groups. These nuclear data libraries for 34, 89, and 190 neutron energy groups are, respectively, hy3418-961a.dat, hy8918-961a.dat, and hy19048-961a.dat. These nuclear data libraries are all based on ENDF/B-VI, release 2, with revised data for U. The "a" indicates that corrections have been applied by Studsvik Scandpower to account for resonance capture effects in ^{238}U.

6. Spectral Calculations and Data Reduction Method Used:

(a) Resonance treatment including mutual shielding (overlap of resonances): HELIOS interpolates library data from tables of group resonance integrals (RIs) for homogeneous mixtures of the resonance isotopes with hydrogen. Nuclides other than hydrogen are represented by intermediate resonance factors λ applied in the background cross section, σ_b. Using this σ_b the RI can be deduced, and the group XS can be determined. In heterogeneous calculations, an equivalence of the flux with that of a homogeneous system is facilitated by adding an equivalence cross section, Σ_e, to the background cross section. In HELIOS, the problem of the interaction of resonance isotopes is handled at two extremes: no interaction, and full interaction. For the full interaction, resonances of different isotopes overlap; such isotopes form a resonance category. A combination of the categories is called a resonance set. There are nine resonance sets available for HELIOS-1.4 calculations. For all these reported results, the HELIOS-1.4 cases were performed with the RES = 4 option (as recommended by Studsvik Scandpower representatives) in the RUN operator. RES signals a user-defined choice of resonance categories. RES = 4 refers to the set with the three categories for ^{238}U, for the rest of heavy metal (HM) nuclides, and for the non-HM nuclides.
(c) Fission spectra: For the fission spectrum calculation, a weighted mix of most of the fissionable nuclides is used (^{234}U, ^{235}U, ^{236}U,^{238}U, ^{237}Np, ^{239}Np, ^{236}Pu, ^{238}Pu, ^{239}Pu, ^{240}Pu, ^{241}Pu, ^{242}Pu) and some average fission spectrum is added to represent the other fissionable actinides.
(d) The (n,2n) reaction: In the HM burnup calculations (chain), the (n,2n) reactions for ^{232}Th, ^{233}U, ^{238}U, and ^{244}Cm are considered. In addition, (n,3n) reactions are considered for ^{232}Th, ^{233}U, ^{234}U, and ^{238}Pu.

7. Number of Energy Groups Used in the Different Phases:

The final ORNL VENUS-2 benchmark results from the cell calculations and from the core calculations were performed using 190 neutron energy groups. Calculations for interest, corroboration, and comparisons were also performed with 34 energy groups and 89 energy groups. See Item 10 of this benchmark summary for further details of the additional 34-group and 89-group results, compared to the official ORNL 190-group results.

8. Calculations:

(a) Type of calculation: heterogeneous
(b) Theory used: transport theory
(c) Method used: Current coupling (between structures) and collision probability (within structures); this is known as the CCCP methodology.
(d) Calculation characteristics: A very detailed model was used for the final ORNL VENUS-2 core representation. The "windmill" pattern was used in modeling the moderator region surrounding each fuel pin. Explicit fuel-cladding gaps were used in the model of the UO_2 fuel pins, while the MOX fuel pins did not have a fuel-cladding gap. For the core calculations, the current coupling parameter k = 4 was used as recommended.

9. Other Assumptions and Characteristics:

The final ORNL VENUS-2 HELIOS model (from which the ORNL reported results come) includes the following confirmed assumptions: The Pyrex assemblies are modeled with void within the inner radius of the Pyrex and void between the outer Pyrex and inner cladding radii.

Water surrounds the Pyrex assembly outer cladding radius. The central square hole within the inner baffle wall is modeled to be entirely water. Spectral reflection boundary conditions are applied at the symmetry boundaries. For the HELIOS core calculations, the VENUS-2 model assumes a very small specific power level of 0.0009141 W/gHE.

10. Comments Useful for Correctly Interpreting the Results:

For the tables for the CELL CALCULATIONS, the isotopes ^{234}U and ^{236}U were added by me to those in the sample tables from the VENUS-2 benchmark specifications, Appendix 3 of NEA/SEN/NSC/WPPR(99)2. These uranium isotopes are necessary for the complete reaction rate details; ^{238}Pu, on the other hand, is not needed, as it is not explicitly in any of the modeled fuel compositions. The reaction rates presented in the tables are normalized in the cell calculation tables such that the sum (over all energy groups and for all the participating nuclides) of the fission rates for each case is numerically 1.87×10^8. For the absorption rates and fission rates, the three energy groupings chosen are closest to those requested in the benchmark specifications: these are defined as neutron energies above 4.881 keV, between 4.881 keV and 3.928 eV, and below 3.928 eV.

For the VENUS-2 CORE CALCULATIONS, the relative pin power distributions are normalized such that the total of 640 fuel pins in one-quarter of the core have a total sum of relative pin powers of 640. The tabulated pin powers represent one-eighth of the core, but with the full "diagonal sites" (numbers 6, 13, 21, 30, 38, 49, 61, 73, 85, and 100) fuel pins included.

All of the cell calculations and core calculations presented in my final VENUS-2 benchmark results are from HELIOS-1.4 cases using 190 neutron energy groups. The results obtained using 89 and 34 neutron energy group libraries with HELIOS-1.4 are similar with a few differences. Some of the interesting data are shown below from different calculations for the same VENUS-2 model (the final one) using different numbers of neutron energy groups. One can see that k_{eff} is very similar for 190 and 89 groups, but that the k_{eff} value for 34 groups is larger.

Core calculations (k_{eff}) as function of number of energy groups

Number of energy groups	k_{eff} (as calculated with HELIOS-1.4)
190	0.99870
89	0.99907
34	1.00150

The relative pin powers (for certain pin locations) from three different HELIOS-1.4 cases for the same final VENUS-2 model but using 190, 89, and 34 neutron energy group nuclear data libraries are shown below. The pin locations are identified by the pin numbering scheme (1–325) as shown at TFRPD2. The chosen pin locations are seemingly interesting places at the inner and outer baffle walls, at the position of the hottest observed fuel pin power level, near some of the Pyrex sites, and in the center of the fuel array.

Comparison of certain relative pin power values from core calculations with different number of energy groups

	190 groups	89 groups	34 groups
1	1.04232	1.03684	1.03189
5	1.15284	1.14779	1.14311
6	1.29802	1.29296	1.28756
23	1.27493	1.27130	1.26559
34	1.34733	1.34475	1.33970
68	1.29560	1.29428	1.29042
69	1.30816	1.30712	1.30384
85	1.17368	1.17340	1.17192
100	0.91350	0.91320	0.91290
101	1.54459	1.54345	1.54093
229	0.78515	0.78708	0.79075
311	0.42566	0.42690	0.43035
325	0.21713	0.21682	0.21796

Cell calculations (k_{inf}) for different number of energy groups

Number of energy groups	3.3 UO_2	2.0/2.7 MOX	4.0 UO_2
190	1.40847	1.26254	1.34333
89	1.40677	1.26279	1.34152

Page Intentionally Blank

INTERNAL DISTRIBUTION

1. B. B. Bevard
2. S. M. Bowman
3. B. L. Broadhead
4. R. L. Childs
5. E. D. Collins
6. B. S. Cowell
7. M. D. DeHart
8. F. C. Difilippo
9. K. R. Elam
10–14. R. J. Ellis
15. S. E. Fisher
16. I. C. Gauld
17–21. J. C. Gehin
22. S. R. Greene
23. T. W. Horning
24. D. T. Ingersoll
25. H. T. Kerr
26. M. A. Kuliasha
27. R. A. Lillie
28. S. B. Ludwig
29. G. E. Michaels
30. D. L. Moses
31. C. V. Parks
32–36. R. T. Primm III
37. W. J. Reich
38. I. Remec
39. C. E. Sanders
40. D. J. Spellman
41. C. C. Southmayd
42. J. C. Wagner
43. R. M. Westfall
44. G. L. Yoder, Jr.
45. Central Research Library
46–47. ORNL Laboratory Records (OSTI)
48. ORNL Laboratory Records (RC)

EXTERNAL DISTRIBUTION

49. M. L. Adams, Department of Nuclear Engineering, Texas A&M University, Zachry 129, College Station, TX 77843
50. D. Alberstein, Los Alamos National Laboratory, MS-K551, P.O. Box 1663, Los Alamos, NM 87545
51. P. Alekseev, Russian Research Center “Kurchatov Institute,” Department of Physical and Technical Research of Advanced Reactors, Kurchatov Square, 1, 123182 Moscow, Russia
52. J. B. Briggs, Idaho National Environmental and Engineering Laboratory, P.O. Box 1625-3855, Idaho Falls, ID 83415-3855
53. M. S. Chatterton, U.S. Nuclear Regulatory Commission, Office of Nuclear Reactor Regulation, MS O10 B3, Washington, DC 20555-0001
54. K. Chidester, Los Alamos National Laboratory, MS-E502, P.O. Box 1663, Los Alamos, NM 87545
55. R. H. Clark, Duke/Cogema/Stone & Webster, 400 South Tyrone Street, WC-32G, P.O. Box 1004, Charlotte, NC 28202
56. W. Danker, U.S. Department of Energy, NN-62, 1000 Independence Avenue SW, Washington, DC 20585

57. M. Delpech, CEN Cadarache, SERSI/LECC, Bat. 212, F-13108, St. Paul les Durance Cedex, France
58. P. J. D'Hondt, SCK-CEN, 200 Boeretang, B-2400, Mol, Belgium
59. N. Fletcher, Office of Fissile Materials Disposition, U.S. Department of Energy, NN-63, 1000 Independence Avenue SW, Washington, DC 20585
60. T. Gould, Lawrence Livermore National Laboratory, P.O. Box 808, MS-L186, Livermore, CA 94551
61. K. Hesketh, British Nuclear Fuels plc, Research and Technology Department, B709, Springfields, Salwick, Preston, Lancashire, PR4 OXJ, U.K.
62. U. Hesse, Gesellschaft fuer Anlagenund Reaktorsicherheit Forschungsgelaende, Postfach 1328, Garching, Germany
63. L. Jardine, Lawrence Livermore National Laboratory, P.O. Box 808, MS-L166, Livermore, CA 94551

64–68. A. Kalashnikov, Institute of Physics and Power Engineering, 1 Bondarenko Square, Obninsk, Kaluga Region, Russia 249020

69. M. A. Kalugin, Russian Research Center "Kurchatov Institute," Institute of Nuclear Reactors, VVER Division, VVER Physics Department, 123182, Kurchatov Square, 1, Moscow, Russia
70. U. Kasemeyer, Paul Scherrer Institute (PSI), CH-5232 Villigen, Switzerland
71. K. Kitagawa, Representative Director, Nuclear Fuel Industries Ltd., Europe Office, 11 rue Christophe Colomb, 75008, Paris, France
72. D. E. Klein, Associate Vice Chancellor for Special Engineering Programs, The University of Texas System, 210 West Sixth Street, Austin, TX 78701
73. R. W. Lee, Office of Nuclear Reactor Regulation, MS O10 B3, U.S. Nuclear Regulatory Commission, Washington, DC 20555-0001
74. T. Maldague, Belgonucleaire S. A., Avenue Ariane 4, B-1200, Bruxelles, Belgium
75. M. Mattes, Universitaet Stuttgart, Institut fuer Kernenergetik und Emergiesysteme, Postfach 801140, D-70550, Stuttgart 80, Germany
76. B. C. Na, OECD/NEA Data Bank, 12 Bd des Iles, 92130 Issy-les-Moulineaux, France
77. S. Nesbit, Duke/Cogema/Stone & Webster, 400 South Tryon Street, WC-32G, P.O. Box 1004, Charlotte, NC 28202
78. J. O. Nulton, Office of Fissile Materials Disposition, U.S. Department of Energy, NN-61, 1000 Independence Avenue SW, Washington, DC 20585
79. J. M. Parotte, Paul Scherrer Institute (PSI), CH-5232 Villigen, Switzerland
80. S. L. Passman, Booz-Allen & Hamilton, 555 13th Street, NW, No. 480E, Washington, DC 20004

81–85. A. Pavlovitchev, Russian Research Center "Kurchatov Institute," Institute of Nuclear Reactors, VVER Division, VVER Physics Department, 123182, Kurchatov Square, 1, Moscow, Russia

86. K. L. Peddicord, Associate Vice Chancellor, Texas A&M University, 120 Zachry, College Station, TX 77843-3133
87. D. Porsch, Siemens Power Generation Group (KWU), Department NBTI, Postfach 3220, D-91058, Erlangen, Germany
88. G. Radulescu, Framatom Cogema Fuels, 1261 Town Center Drive, MS-423, Las Vegas, Nevada 89143
89. W. D. Reece, Texas A&M University, Department of Nuclear Engineering, Zachry 129, College Station, TX 77843-3133
90. E. Sartori, OECD/NEA Data Bank, 12 Bd des Iles, 92130 Issy-les-Moulineaux, France

91. U. Shoop, Office of Nuclear Reactor Regulation, MS O10 B3, U.S. Nuclear Regulatory Commission, Washington, DC 20555-0001
92. E. Siskin, Office of Fissile Materials Disposition, U.S. Department of Energy, MD-1/2, 1000 Independence Avenue SW, Washington, DC 20585
93. J. Thompson, Office of Fissile Materials Disposition, U.S. Department of Energy, MD-4, 1000 Independence Avenue SW, Washington, DC 20585
94. K. Van der Meer, Studie Centrum voor Kernenergie, SCK-CEN, 200 Boeretang, B-2400, Mol, Belgium
95. M. Williams, Louisiana State University, Baton Rouge, LA 70803-5820
96. T. Wolf, Siemens/KWU, Department NBTS, Postfach 3220, Freyeslebenstr. 1, D-91050, Erlangen, Germany
97. A. Worrall, British Nuclear Fuels plc, MOX Design and Licensing, B709 Research and Technology Department, Springfields, Salwick, Preston, Lancashire, PR4 OXJ, U.K.
98. W. Zwermann, Gesellschaft fuer Anlagenund Reaktorsicherheit (GRS) mbH, Forschungsgelaende, D-85748, Garching, Germany